

PHYSICAL REVIEW B

CONDENSED MATTER

THIRD SERIES, VOLUME 50, NUMBER 1

1 JULY 1994-I

Local-density studies of the structure and electronic properties of B and S in an Fe grain boundary

Shaoping Tang and A. J. Freeman

Department of Physics and Astronomy, Northwestern University, Evanston, Illinois 60208-3112

G. B. Olson

Department of Materials Science and Engineering, Northwestern University, Evanston, Illinois 60208

(Received 10 January 1994; revised manuscript received 21 March 1994)

The structure and electronic properties of B and S impurities in an Fe $\Sigma 3[1\bar{1}0](111)$ grain boundary are studied using the DMol molecular cluster method. A large cluster containing 91 atoms is used to simulate the local environment of the boundary. Optimized atomic geometries are obtained by atomic force calculations. The results show that impurities induce large relaxations in the grain boundary, and that the electronic structure of the hybridized B/Fe system is very different from that of the nonhybridized S/Fe system.

I. INTRODUCTION

It is well known that impurities such as P, S, Sn, and Sb cause intergranular embrittlement of Fe, while C and B enhance the intergranular cohesion in iron and alloy steels.¹ Because of its importance to grain-boundary sensitive properties such as the stress-corrosion resistance of ultrahigh-strength steels, the mechanism underlying these phenomena has been the subject of considerable research effort.²⁻¹¹ It has become evident from these studies that the desired understanding will require detailed consideration of precise grain-boundary atomic structure and energetics coupled with underlying electronic level structure and properties.

Recent theoretical efforts have applied first-principles electronic structure calculations to study the role of impurities in the embrittlement of Fe and proved to be very useful in elucidating possible mechanisms of Fe embrittlement.⁶⁻¹⁰ One of the major obstacles in using the first-principles approach, however, has been the need for substantial computing power not available until recently. With the rapid development of computer technology, one can now perform such calculations with reasonable cost.

In a previous paper, we applied the first-principles DMol molecular cluster method to study phosphorus-induced structural changes in the Fe grain boundary (GB).¹⁰ It was shown that P induces large relaxations in the GB, and the electronic structure of the GB also changes significantly. In this paper, we compare the effects of B and S impurities on the Fe $\Sigma 3[1\bar{1}0](111)$

grain boundary using the same theoretical techniques: We first determine the atomic relaxation induced by the impurities using atomic force calculations; the electronic structure is then calculated for the relaxed structure. Previous electronic structure calculations used relatively small clusters³⁻⁷ and did not consider the role of lattice relaxation.^{8,9} Those studies provided useful information on the bonding between the metal and impurities. However, as the large relaxations induced by impurities may also change the electronic structure of the Fe GB, consideration of atomic relaxation is necessary for a correct description of the electronic structure.

II. METHODOLOGY

We use the DMol method¹² which is a first-principles numerical method for solving the local-density-functional equations and is capable of calculating analytic energy gradients¹³ for each atom within the cluster model. The Hedin-Lundqvist exchange-correlation potential¹⁴ is employed with the frozen-core approximation. We use extended basis sets for the B, S, and Fe atoms, i.e., a double set of valence functions plus a single *d* polarization function for B and S atoms and a single *p* function for Fe. The binding energy of a cluster is defined as $E_b = -(E_t - E_a)$ where E_t is the total energy of the cluster and E_a is the sum of atomic total energies. For a given atomic geometry, the binding energy of the system and the forces on atoms of interest are calculated. To find the optimized geometry, the atoms are further dis-

placed according to the forces acting on them. An optimized structure is obtained when all the forces acting on the atoms are sufficiently small. In this work, the degree of self-consistent convergence is measured by root-mean-square (rms) changes in the charge density; it is set to 10^{-5} which allows the total energy to converge to 10^{-5} Ry. The force convergence criterion is 6.0×10^{-3} Ry/a.u.

The grain boundary considered is the $\Sigma 3[1\bar{1}0](111)$ “incoherent” twin boundary as treated in previous studies.^{8–11} The 91-atom cluster model contains 17 layers of Fe adjacent to the grain boundary and is shown in Fig. 1. The impurity atoms are placed at the center of the trigonal prism formed by iron atoms in the GB core, and D_{3h} symmetry is used. In searching for the optimum geometry, the boundary atoms of the cluster are fixed in their bulk positions. When we refer to the relaxation of a particular atom, say, Fe₁₁, other atoms satisfying D_{3h} group operations have the same relaxation as Fe₁₁.

III. RESULTS AND DISCUSSION

A. Atomic relaxation study

The relaxation study is carried out by force calculations in which atoms in columns 1 and 2 in Fig. 1 can relax along the z direction since those atoms are most affected by the impurity in the GB center. For the B/Fe system, we first calculate the relaxation of Fe atoms using a 53-atom cluster which takes less computing time. Since the interlayer distance and the bond length between impurity and Fe atoms are underestimated using the 53-atom cluster as previously shown in the P/Fe system,¹⁰ the result from the small cluster is used as an initial input for the 91-atom cluster calculation. The final optimized structural information is presented in Table I. For the S/Fe system, we use the P/Fe system data for the 91-atom cluster¹⁰ as initial input, anticipating that S and P induce similar relaxations.

The basic relaxation results are (1) For the clean GB

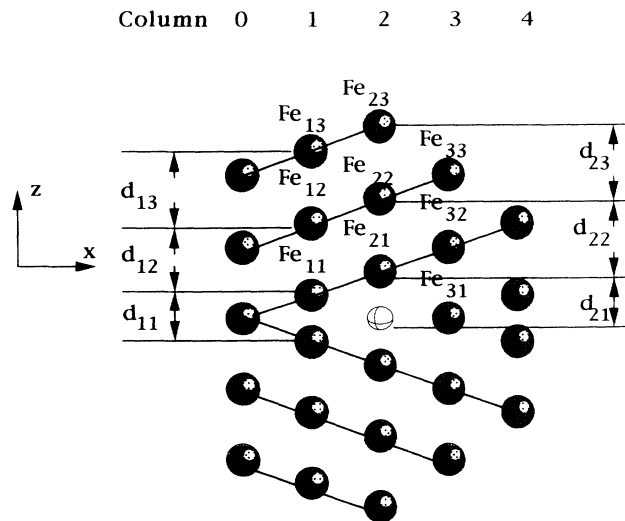


FIG. 1. Side view of the 91-atom cluster simulating the Fe grain boundary. The impurity atom is put in the center of the trigonal prism formed by Fe atoms in the GB core. Atoms in each Fe layer are not shown in the figure.

TABLE I. Calculated structural parameters (in Å) for the 91-atom cluster model defined in Fig. 1. The “initial” distances are calculated from the unrelaxed coincidence site lattice structure. GB-1 refers to the geometry when Fe₂₁ relaxes inward towards the center of the GB and GB-B and GB-S refer to the cases when B and S are added to the GB; d_{Fe} is the distance between the two near-center atoms in column 2 in the pure GB and E_b is the binding energy in eV.

	Initial	GB-1	GB-B	GB-S
d_{11}	1.65	2.49	2.48	2.61
d_{12}	2.48	2.47	2.41	2.35
d_{13}	2.48	2.07	2.14	2.14
d_{21}			2.15	2.35
d_{22}	2.48	2.48	2.46	2.30
d_{23}	2.48	2.93	2.01	1.97
d_{Fe}	3.31	2.43		
E_b		421.86	428.67	426.96

structure, there are two structures having energy minima. One corresponds to the case in which two center Fe atoms (Fe₂₁) move towards the GB center, referred to as GB-1. This gives a structure for the $\Sigma 3$ GB core which is very similar to the ω phase observed in Ti alloys. The other structure corresponds to Fe₂₁ atoms moving apart from the GB center (an “anti- ω ” structure), referred to as GB-2. It has been shown that the GB-1 structure is more stable energetically than the GB-2 structure.¹⁰ Here, we also allow the Fe₃₂ atoms to relax along the z direction in the GB-1 structure. It is found that the calculated results show an average difference of less than 1% for structural data and very small changes for binding energy compared to the GB-1 structure displayed in Table I. Hence, the extra relaxation of the Fe₃₂ atoms causes only slight changes for the clean GB structure. (2) When impurities are introduced in the center of the GB, the Fe atoms directly above the impurity (Fe₂₁ atoms) are pushed outwards from the center (favoring the GB-2 structure), and this affects the atoms in the outer layer. The net effect is that almost all Fe atoms are relaxed outwards from the center. (3) S induces larger relaxation for atoms near the impurity (e.g., d_{11} and d_{21}) than does B as shown in Table I. The Fe atom (Fe₂₁) directly above the impurity relaxes outwards 42% for S/Fe and 30% for B/Fe compared with its initial (unrelaxed coincidence site lattice) position. The bond length between Fe₂₁ and B is 2.15 Å and is a smaller than that between Fe₂₁ and S (2.35 Å).

The relaxation results can be compared with an empirical calculation using a modified embedded-atom method (EAM) by Krasko.¹¹ The EAM calculations show that for the clean GB, the stable structure corresponds to the down position of Fe₂₁ which agrees with our GB-1 structure. After B and S are put in the center of the GB, the EAM also found that S induces larger relaxation of Fe atoms near the impurity than does B. The calculated bond length between Fe₂₁ and B and between Fe₂₁ and S from the EAM are 1.96 and 2.60 Å, respectively, which has an average difference of 10% with the results of the present calculation. Our bond length value for Fe₂₁ and S (2.35 Å) may increase if an even larger cluster is used. As can be seen from Table I, the distance between the boundary atoms and the nearest inner atoms in the z

direction are compressed (i.e., d_{13} and d_{23}) compared to the bulk value of 2.48 Å. It is quite possible that the boundary atoms will be pushed further outwards when a larger cluster is used. If that is true, we can expect a weakening of the vertical interaction between Fe_{21} and S.

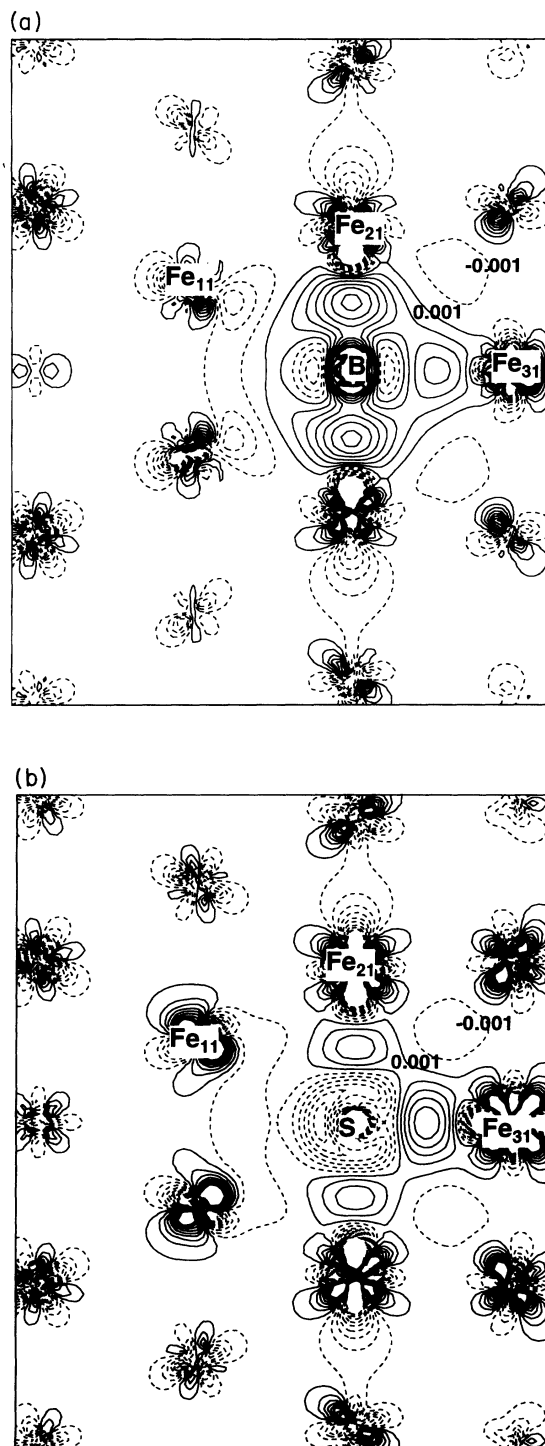


FIG. 2. Charge-density difference between impurity in the GB and a superposition of a single impurity and pure GB calculated from the 91-atom cluster. The plots are in a plane containing the impurity, Fe_{11} , Fe_{21} , and Fe_{31} atoms. The contour spacings are $0.002e/(\text{a.u.})^3$. Solid lines mean a gain of charge, and dashed lines mean a loss of charge. (a) B/Fe and (b) S/Fe.

This may be useful in elucidating the mechanism of S embrittlement since the competition between bonding in the vertical and horizontal directions is an important factor.

It is worth mentioning that although B is a light element, it has a higher binding energy (1.71 eV) in the Fe GB than does S. This is due to the shorter Fe_{21} and B bond length that results in the stronger interaction between B and Fe. Similar results were obtained for the binding energy of B and S in Ni by Painter and Averill⁶ which showed that B binds in the Ni host much more strongly (7.0 eV) than does S (2.2 eV) and produces a smaller expansion of the host cluster than does S.

B. Charge density

Figure 2 shows the charge-density difference plotted in the $(1\bar{1}0)$ plane containing the impurity and several neighboring Fe atoms. (The charge-density difference is calculated by subtracting from the charge density of the impurity in the GB, the pure GB charge density and a

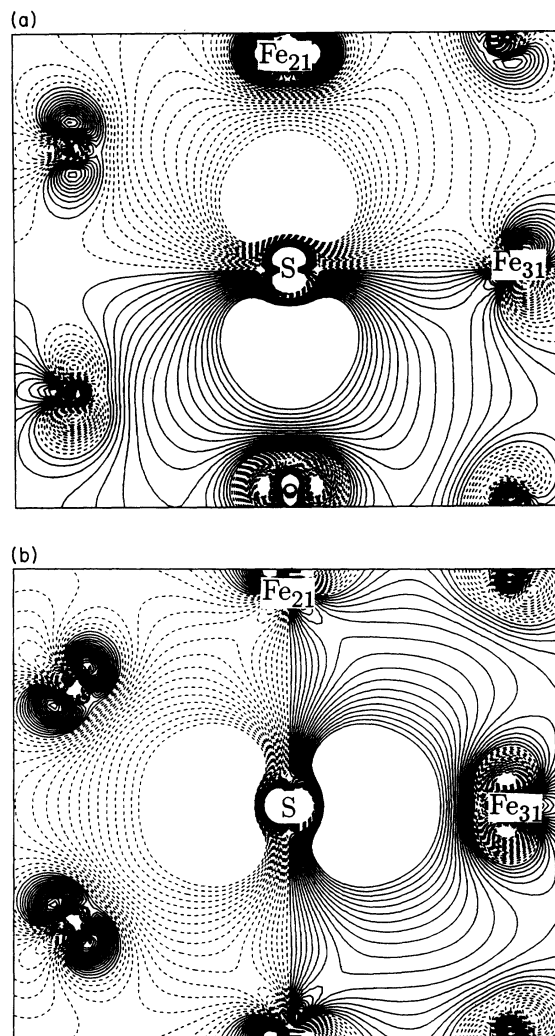


FIG. 3. Contour plot of molecular orbitals for S in the Fe GB. The contour spacing is 0.004. (a) $1A_2'$ orbital; and (b) $1E'$ orbital.

single impurity charge density placed at the center of the GB so that the impurity-induced charge redistribution can be seen more clearly.) Comparing the charge-density difference between the B/Fe and S/Fe systems, we can see that there is one common feature for the two systems: the interaction of impurity and Fe atoms is restricted to a local region near the impurity, although the lattice relaxation is known to extend beyond this area.¹¹

The main difference between them is the charge distribution in the vertical (z) and horizontal (x) directions. In Fig. 2(a), B is seen to form relatively strong covalent-like bonding states with Fe atoms in the vertical direction and a much weaker bonding with Fe atoms in the horizontal direction. In the S/Fe system [see Fig. 2(b)], slightly more charge is accumulated in the region between S and Fe₃₁ atoms than between S and Fe₂₁ atoms, giving the impression that the bonding along the horizontal direction is stronger than that along the vertical direction, although the distance between S and the Fe atoms in both directions are almost equal. The same phenomenon was found for the P/Fe system calculated both from the full-potential linearized augmented-plane-wave⁹ and DMol (Ref. 10) method. It is doubtful that these charge accumulations represent strong covalent bonding between S and Fe since the density of states calculated for S/Fe does not confirm the hybridization between S and Fe.

To understand this, we plot the two molecular orbitals containing mainly S $3p$ electron contributions in Figs. 3(a) and 3(b). In Fig. 3(a), one can see a dominant $S 3p_z$ -like wave function having only weak bonding with Fe₃₁; a similar dominant $S 3p_x$ -like wave function is seen in Fig. 3(b). Hence, the bonding between S and Fe is weak. If we compare Fig. 3 with the free atom S $3p$ wave function (not shown here), we find that the free S $3p$ wave function has greater spatial expansion. When S is in the Fe GB environment, the S- $3p$ electrons will feel the repulsive interaction of nearby Fe electrons and shrink towards the S nucleus, and so there is some charge accumulation in the region between the Fe and S atoms. By contrast, B is found to form a σ -type bonding state with Fe atoms in the vertical direction. This is reflected in Fig. 4 where the $10A_2''$ orbital which is located 2.82 eV below E_F is plotted. It is clearly seen that there is hybridization between B $2p_z$ and Fe $3d_{z^2}$ electrons that is not found in the S/Fe system.

Finally, we note that the charge accumulation in the

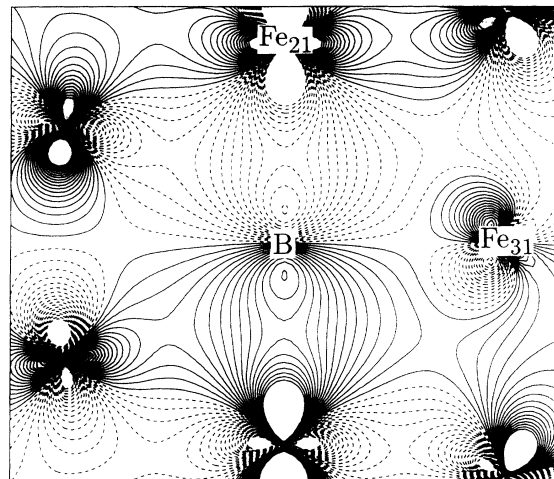


FIG. 4. Contour plot of the $10A_2''$ molecular orbital for B in the Fe GB. The contour spacing is 0.004.

region between S and Fe is accompanied by a decrease of charge in the S center region as can be seen from Fig. 2(b). To estimate how the charges are distributed, we calculate the Mulliken electron population; the results show that there is about $0.37e$ charge redistribution from S $3s$ and S $3p$ states to the high energy S $3d$ state. This will reduce the charge in the center region compared to the free S atom which results in the image of Fig. 2(b).

In summary, we have performed first-principles local-density DMol molecular cluster calculations on the role of the B and S impurities in the Fe grain boundary. When impurities are placed in the center of the GB, it is found that B induces less relaxation for nearby Fe atoms than does S. The nearest distance between B and Fe and between S and Fe are 2.15 and 2.35 Å, respectively. For the bonding between impurities and Fe, we found that B $2p_z$ forms a relatively strong σ bonding with Fe₂₁ $3d_{z^2}$, while S has very little hybridization with Fe, resulting in a weak bonding state. These differences in electronic structure for B and S may be useful in understanding their different effects on grain-boundary cohesion.

ACKNOWLEDGMENTS

This work was supported by the Office of Naval Research (Grant No. N00014-90-J-1363), and by a computing grant at the Pittsburgh Supercomputing Center, supported by the NSF Division for Advanced Scientific Computing.

¹G. B. Olson, in *Innovations in Ultrahigh-strength Steel Technology*, edited by G. B. Olson, M. Azrin, and E. S. Wright, Proceedings of Sagamore Conference, No. 34 (Sagamore Army Material Research Conference, Lake George, New York, 1987), p. 3 and references therein.

²J. R. Rice and J.-S. Wang, *Mater. Sci. Eng.*, A **107**, 23 (1989).

³R. P. Messmer, *Phys. Rev. B* **23**, 1616 (1981).

⁴R. P. Messmer and C. L. Briant, *Acta Metall.* **30**, 457 (1982).

⁵A. Collins, R. C. O'Handley, and K. H. Johnson, *Phys. Rev. B* **38**, 3665 (1988).

⁶G. S. Painter and F. W. Averill, *Phys. Rev. Lett.* **58**, 234 (1987).

⁷M. E. Eberhart and D. D. Vvedensky, *Phys. Rev. Lett.* **58**, 61 (1987).

⁸G. L. Krasko and G. B. Olson, *Solid State Commun.* **76**, 247 (1990).

⁹R. Wu, A. J. Freeman, and G. B. Olson, *J. Mater. Res.* **7**, 2403 (1992).

¹⁰S. Tang, A. J. Freeman, and G. B. Olson, *Phys. Rev. B* **47**, 2441 (1993).

¹¹G. L. Krasko, in *Structure and Properties of Interfaces in Materials*, edited by W. A. T. Clark, U. Dahmen, and C. L. Briant, MRS Symposia Proceedings No. 238 (Materials Research Society, Pittsburgh, 1991), p. 481.

¹²B. Delley, *J. Chem. Phys.* **92**, 508 (1990).

¹³B. Delley, *J. Chem. Phys.* **94**, 7245 (1991).

¹⁴L. Hedin and B. I. Lundqvist, *J. Phys. C* **4**, 2064 (1971).

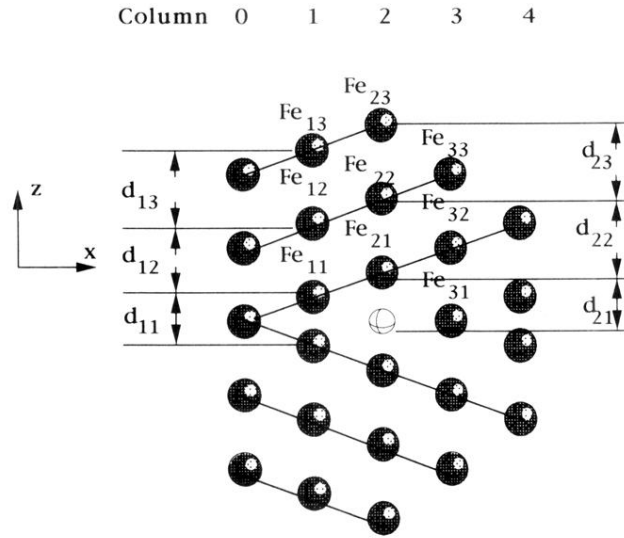


FIG. 1. Side view of the 91-atom cluster simulating the Fe grain boundary. The impurity atom is put in the center of the trigonal prism formed by Fe atoms in the GB core. Atoms in each Fe layer are not shown in the figure.